Neutron reflectivity studies of critical adsorption: Behavior of the surface scaling function

James Bowers
Department of Chemistry, University of Exeter, Stocker Road, Exeter EX4 4QD, United Kingdom

Ali Zarbakhsh
Department of Chemistry, Queen Mary, University of London, Mile End Road, London E1 4NS, United Kingdom

Hugo K. Christenson*
School of Physics and Astronomy, The University of Leeds, Leeds LS2 9JT, United Kingdom

Ian A. McLure
Department of Chemistry, The University of Sheffield, Sheffield S3 7HF, United Kingdom

John R. P. Webster
ISIS Facility, CLRC Rutherford Appleton Laboratory, Chilton, Didcot, Oxon OX11 0QX, United Kingdom

Roland Steitz
Berlin Neutron Scattering Center, Hahn-Meitner-Institut, Glienicker Strasse 100, D-14109 Berlin, Germany
(Received 22 July 2005; published 28 October 2005)

Neutron reflectometry has been employed to examine the nature of the critical adsorption surface scaling function for a near-critical mixture of hexane-d_{14}+perfluorohexane adsorbing to a solid substrate from the liquid one-phase region. The analysis method of Dietrich and Schack has been applied to examine the nature of the power-law part of the critical adsorption surface scaling function, which has been found to behave as $m(z) \sim P_0 z^{-\mu}$ as the critical point is approached. Values of $\mu = 0.514 \pm 0.018$ and $P_0 = 0.90 \pm 0.04$ have been obtained. These values are consistent with theoretical expectations ($\mu^{\text{th}} = 0.516 \pm 0.004$; $P_0^{\text{th}} = 0.94 \pm 0.05$), the value determined from Monte Carlo simulations ($P_0^{\text{MC}} = 0.866$), and other experimental determinations ($P_0^{\text{ex}} = 0.955 \pm 0.08$).

DOI: 10.1103/PhysRevE.72.041606 PACS number(s): 68.08.De, 61.12.Ha, 68.35.Rh, 68.43.Fg

I. INTRODUCTION

Many wetting and adsorption phenomena can be accessibly examined at the interface between an inert substrate, be it vapor, liquid or solid, and a binary liquid mixture [1,2]. In the liquid two-phase region of a partially miscible mixture, a transition from partial to complete wetting of the substrate occurs at a temperature T_W below the critical temperature T_C, such that a macroscopic film of the phase rich in the preferentially adsorbed component interposes itself between the substrate and the second liquid phase. In the liquid one-phase region, the nature of the adsorption depends on distance from the critical point, which may be defined as $t_{CP} = |T_C - T_0|/T_C$, where T_0 is the coexistence temperature for the composition of the particular mixture. If T_C is approached along a path with $t_{CP} = 0$, i.e., a mixture with critical composition, composition fluctuations in the bulk amplify the surface excess of the preferentially adsorbed component and critical adsorption occurs [3,4]. Close to the critical point, along a path with $t_{CP} = 0$ the surface excess diverges as $\Gamma_{CA} \sim t^{-0.305}$ where $t = |T - T_C|/T_C$. Along this path the nature of the composition profile is generally well known from both experimental and theoretical approaches [1,6]. The composition profile displays power law decay $\sim z^{-\mu}$, where z is the coordinate normal to the interface and the theoretical value of the exponent μ is $\mu^{\text{th}} = 0.516$, close to the substrate and exponential decay further into the bulk mixture. The crossover between these two behaviors occurs at a length scale set by the correlation length of the composition fluctuations, ξ. Recent experimental effort has concentrated on examining amplitude ratios [7–13] and the nature of strong and weak critical adsorption [14–18]. (Strong critical adsorption means that the surface is saturated with the preferentially adsorbed component and weak critical adsorption that the primary adsorption layer contains both components). A detailed inspection of the composition profile using neutron and x-ray reflectometry [19–23] has also been carried out. For cases where $t_{CP} \neq 0$ the surface excess and composition profile behavior have received considerably less attention. A crossover from critical adsorption to complete wetting is expected [24,25], with the crossover occurring increasingly further from liquid-liquid coexistence with increasing t_{CP}. In our ongoing work we are addressing this shortfall of information and have examined cases where t_{CP} is nonzero [26,27]. In particular we have chosen to examine adsorption from mixtures of hexane-perfluorohexane to chemically modified (e.g., by a coupled octadecyl layer) silicon substrates.

Neutron reflection can provide complementary structural information to ellipsometry, but it has only recently emerged as a means of studying critical and related adsorption phenomena [19–23]. Since neutron reflection is sensitive to the gradient of the composition profile, a stringent test of the

*Author to whom correspondence should be addressed. Electronic mail: phy6hkc@phys-irc.leeds.ac.uk

commonly accepted scaling forms for the critical adsorption composition profile can be made, as shown by a few recent examples [19,20]. Since neutron reflection is applicable at solid–liquid interfaces, concerns regarding component volatility and the effect of liquid-vapor menisci on the measured reflectivity are circumvented. Furthermore, for certain systems isotopic substitution can be employed to enhance the sensitivity of the structure determination. The ability to readily establish near-surface structure, and hence the composition of the layer adsorbed adjacent to the substrate, could also prove useful for the investigation of strong or weak field adsorption.

As a point of reference for the examination of the crossover from critical adsorption to complete wetting, the nature of the critical adsorption is required. Jestin *et al.* [19] have examined critical adsorption at the free surface of the hexane-perfluorohexane mixture and their results suggest that the nature of the scaling laws describing the composition profile for strong-field adsorption may be questionable. In order to explore this result, to obtain reference critical adsorption data, and to attempt to resolve uncertainties in the values of certain universal parameters that describe critical adsorption, we examine here the adsorption from a hexane-d_{14}+perfluorohexane mixture to an octadecyl-coated silicon substrate, which is representative of a strong-field adsorption system because of the strong preferential adsorption of hexane-d_{14}. For appropriate potential gradients the reflectivity close to the total reflection edge can be used to *uniquely* determine the universal amplitude and exponent describing the algebraic decay of the critical adsorption profile [28]. The chosen system possesses a scattering length density profile $(dNb(z)/dz)<0$, where $z>0$ corresponds to the liquid side of the interface, which is an appropriate potential gradient for the Dietrich-Schack analysis and thus allows ready access to the determination of the relevant parameters related to the scaling laws (see Results and Discussion).

II. EXPERIMENTAL SECTION

A. Sample preparation and environment

Hexane-d_{14} (ACROS, 99+D at. %) and perfluorohexane (Lancaster, 98% *n*-isomer) were distilled then refrigerated prior to use. A mixture with volume fraction $\phi=\phi_C=0.50$ ($t_{CP}=0$) was prepared by mass. The experimental cell is similar in design to that we have previously used [26,27] and consists of a trough (unpolished silicon) sealed against a silicon substrate using a Viton O-ring. This sealed unit was then sandwiched between two brass thermostat plates with internal baffles whose temperature was controlled by circulating fluid from a thermostatted circulating bath. Care was taken to ensure that bubble-free liquid sample was introduced into the sealed sample cavity through the filling holes accessed via greaseless plug valves. The silicon block (Crystran) was 10 mm thick with diameter=100 mm. The phase-separation temperature for the mixture was established by viewing a sample contained in a jacketed glass ampoule, the jacket being thermostatted by the same circulating bath controlling the cell temperature. The surface of substrate was treated with the silane coupling agent octadecyltrichlorosilane (ACROS, 95%) using established methods [26]. The sample temperature was monitored using a platinum resistance thermometer (Pt100) inserted in to the trough section of the cell. The temperature control and homogeneity were better than ±0.03 K.

B. Neutron reflection measurements

Neutron reflectivity measurements were performed on the V6 reflectometer at the BERII reactor at the Hahn-Meitner-Institut, Berlin, Germany. A horizontal beam of monochromatic neutrons with wavelength $\Lambda=4.66$ Å (±3%) was transmitted through the silicon block and incident at the silicon-liquid interface with a grazing angle θ. V6 was operated in a θ-2θ geometry with a vertical scattering plane. The cell was carefully aligned before each measurement at all temperatures studied by performing a series of rocking and table height scans. After each temperature change a short equilibration time was allowed before checking the alignment of the cell. At no time did the cell alignment drift beyond the realms of the accepted experimental error ($|\delta\theta| < 0.005°$). Between changing temperature and starting the collection of the reflectivity data a period of typically one hour elapsed. The reproducibility of the measurements was confirmed by recovering the same reflectivity upon cycling the temperature both upwards and downwards for a few chosen temperatures.

In a neutron reflection experiment [29], the reflectivity, R, is measured as a function of momentum transfer normal to the interface, $Q=4\pi \sin\theta/\Lambda$. The reflectivity data were corrected for illuminated area and the background was subtracted before model fitting was performed. Model fits were obtained using the Parratt32 data analysis program [30] with the reflectivity calculated using Parratt's method [31]. Standard optical layer models are employed to calculate the reflectivity from a scattering length density profile $Nb(z)$, where N is the number density of nuclei, b is the average bound coherent scattering length per nucleus, and z is the coordinate normal to the interface. The composition is related to the scattering length density through $Nb=\Sigma_i \Phi_i (Nb)_i$, where Φ_i and $(Nb)_i$ are the volume fraction composition and scattering length density, respectively, of component i. The model of the surface used includes a silicon substrate, a silicon oxide layer, an octadecyl layer, and a layer representing the primary adsorbed film. The $Nb(z)$ profile used in the reflectivity calculation is constructed from a set of layers (typically 200) each, of thickness (typically 2–5 Å) appended to the primary layer; the Nb of each layer is calculated according to the proposed functional form for $Nb(z)$.

C. Phase diagram and correlation length

The phase diagram for the hexane-d_{14}+perfluorohexane mixture has been reported previously [27]. This diagram is not as complete as desired owing to the high cost of the materials coupled with problems associated with their volatility and the necessity to work with small quantities. The separation temperature, T_0, for the sample studied here is known, but for the analysis reference to a more complete

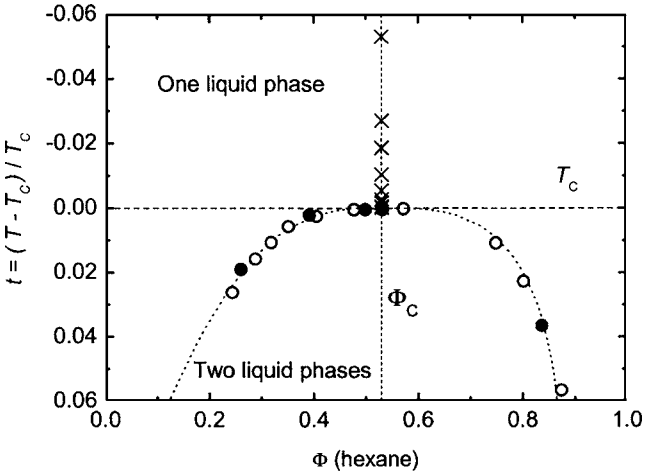

FIG. 1. Phase diagram (t-Φ) for hexane perfluorohexane. The dotted curve is the coexistence curve for hexane-h_{14} perfluorohexane fitted according to Wegner's extended scaling formula [33,34]. Data from Bedford and Dunlap [35] for hexane-h_{14} perfluorohexane (○); data for hexane-d_{14} perfluorohexane (●).

coexistence curve is required. To provide the required coexistence curve we have resorted to a different approach. The T-ϕ representation of the phase diagram returns very symmetrical coexistence curves and Munson [32] noted that when plotted as T_0/T_c against ϕ the coexistence data for a number of alkane-perfluoroalkane mixtures fell on a common curve. Furthermore, the generality of this can be extended to dimethylsiloxane-perfluoroalkane mixtures [33]. The coexistence curve for hexane-h_{14}–perfluorohexane can be represented using Wegner's extended scaling method [33,34], and the resulting curve is shown in Fig. 1 together with experimental coexistence data [35]. Thus the Wegner-derived curve can be assumed to be "universal" for the mixtures concerned. A few measured points for the hexane-d_{14}–perfluorohexane mixture have been included on Fig. 1 and demonstrate the accuracy of the method for the present liquid mixture. Close to the critical point, the order parameter defined by the coexistence curve can be represented as $\Phi_F - \Phi_H = m_0 t^\beta$, where $\beta = 0.325$, $\Phi_F(\Phi_H)$ are the volume fraction compositions of the perfluorohexane- (hexane-) rich phases and $m_0 = 1.888$ for the hexane-perfluorohexane mixture.

The correlation length dependence on t, described by $\xi = \xi_0 t^{-\nu}$, where $\nu = 0.632$, has been reported for the hexane-h_{14}–perfluorohexane system [19,36–38] and amplitudes of $\xi_0 = 2.0 \pm 0.2$ Å, 2.2 ± 0.1 Å, 3 ± 1 Å, and 5.5 ± 1.5 Å have been found. The appealing assumption that the amplitude of the correlation length is unaffected by isotopic substitution may be of doubtful validity. Jestin *et al.* [19] record different amplitudes for methanol-cyclohexane mixtures with different isotopic labelling. However, this may be attributed to the notorious ability of this mixture to absorb water and thus alter its phase behavior. The correlation length amplitude has been retained as a modelling parameter but with its magnitude guided by the reported values.

D. Characterization of substrate and primary adsorbed layer

The surface was characterized by measuring reflectivities from Si–hexane-h_{14}, Si–hexane-d_{14}, and Si-perfluorohexane interfaces, allowing the thickness, roughness and scattering length density of the silicon oxide layer and the coupled octadecyl layer to be established, together with the degree of solvent ingress into the coupled layer. The oxide layer was not characterized prior to attachment of the coupled layer since the structure of the oxide layer may alter as a consequence of the cleaning and coupling procedures. The oxide layer on the Si block was found to be 8 ± 2 Å thick. No roughness, at either the Si-oxide interface or at the oxide–coupled-layer interface, was necessary, probably as a consequence of the utilizable Q range. The Nb of the oxide layer was $(3.5 \pm 0.2) \times 10^{-6}$ Å^{-2}. It was found that the solvated octadecyl layer was of thickness ~24 Å (no roughness required). The octadecyl layer region appeared to be composed of ~68 vol % coupled alkyl chains and ~32 vol % ingressed solvent, and these proportions did not vary with the identity of the solvent. The primary adsorbed layer, i.e., the layer immediately abutting the coupled octadecyl layer, was modelled with the choice of thickness $d_1 = 10$ Å and scattering length density $Nb_1 = 5.5 \times 10^{-6}$ Å^{-2}. These parameters were determined at the temperature furthest from T_C ($\Delta T = T - T_C = 15.3$ K) to remove, as far as possible, the influence of critical adsorption. The parameters used in the analysis are given in Table I.

III. RESULTS AND DISCUSSION

The measured reflectivity data are displayed in Fig. 2(a). The inset to Fig. 2(a) shows the subtle but distinct changes in the reflectivity in the region close to the critical edge, located at $Q = Q_C \approx \sqrt{16\pi \Delta Nb}$, where ΔNb is the difference in scattering length density of the two bulk phases, i.e., silicon and the liquid mixture. The reflectivity data have been analyzed using two different methods. First, the critical adsorption scaling function expected to be obeyed along the trajectory on the phase diagram followed in these measurements has been used to fit the experimental reflectivity curves. Optical layer models have been used to represent the $Nb(z)$ profiles. Second, key parameters describing the composition profile close to T_C have been uniquely determined using the method of Dietrich and Schack [28].

A. Scaling functions

The surface order parameter is defined as $m(z) = \Phi(z) - \Phi_B$, where $\Phi(z)$ is the local volume fraction composition at location z, and Φ_B is the volume fraction of the bulk liquid mixture. Considering only critical adsorption in the one-liquid (+) phase region, $m(z)$ can be represented as $m(z) = m_0 t^\beta G(x,y)$, where $G(x,y)$ is the surface scaling function. If the interfacial free energies, σ_i, of the two mixture components ($i = 1,2$) against the substrate are very different, i.e., $\Delta\sigma = |\sigma_1 - \sigma_2| \gg 0$, then one component saturates the surface and *strong* critical adsorption occurs [17,18]. The important variables are $x = z/\xi$ and $y = \mathbf{h}_1 t^{-\Delta_1}$ which are, respectively, a dimensionless length scale and a dimensionless surface field, where $\Delta_1 = 0.464$ and $\mathbf{h}_1$ is proportional to the magnitude of $\Delta\sigma$. In the strong-field regime $G(x,y) \cong P(x)$ and the limiting asymptotic forms of $P(x)$ are $P(x) = P_0 x^{-\beta/\nu}$ for $x \to 0$ and

TABLE I. Summary of parameters employed in the data analysis using Eq. (2).

Substance	Scattering length density[a] Nb (10^{-6} Å^{-2})	Fit parameters for Eq. (2)
silicon	2.07	$P_0=0.94$
silicon oxide	3.6[b]	$c=0.95$
octadecyl-chain	−0.5[b]	$\xi_0=2.4$ Å
hexane-d_{14}	6.08[c]	$\Delta Nb_0=2.54\times10^{-6}$ Å^{-2}
perfluorohexane	3.54	$m_0=1.888$
bulk mixture	4.81	$z_e=50$ Å$(t<1.70\times10^{-3})$
		$z_e=65$ Å$(t\geqslant1.70\times10^{-3})$

Additional parameters used in the optical-layer models

Layer	Thickness d (Å)	Scattering length density[a] Nb (10^{-6} Å^{-2})
silicon oxide	8	3.50
octadecyl	24	1.60
Primary/ad-layer	10	5.50

[a]Calculated at 25 °C.
[b]Estimated or determined by modeling.
[c]Calculated assuming 99 D at. %.

$P(x)=P_\infty\exp(-x)$ for $x\to\infty$. An appropriate and established form for $P(x)$ that accommodates these limits is [5]

$$m(z)=m_0P_0t^\beta\left(\frac{\xi}{z+z_e}+c\right)^{\beta/\nu}\exp\left(-\frac{z+z_e}{\xi}\right),\qquad(1)$$

where the parameter $c\approx1$ serves to define the crossover from algebraic to exponential decay, i.e., if $c\ll1$ power law decay dominates. The extrapolation length, z_e, is necessary to maintain a sensible composition profile local to the substrate at small z. After translation into terms of neutron scattering length densities Eq. (1) becomes

$$Nb(z)=At^\beta\left(\frac{\xi}{z+z_e}+c\right)^{\beta/\nu}\exp\left(-\frac{z+z_e}{\xi}\right)+Nb_\mathrm{B},\qquad(2)$$

where Nb_B is the bulk mixture scattering length density, and Eq. (2) has been used to model the neutron reflection data. Table I summarizes the main parameters used in this analysis. The amplitude A is given by $A=m_0\Delta Nb_0P_0$, where ΔNb_0 is the appropriate conversion factor for changing the order parameter from being defined in volume fraction to scattering length density terms, m_0 is as given earlier; $\Delta Nb_0=2.5\times10^{-6}$ Å^{-2}, which is the difference in scattering length densities of the pure mixture components; $P_0=0.94$ is set at the theoretical value $P_0{}^\mathrm{th}=0.94\pm0.05$. ΔNb_0 is evaluated by solving $Nb_\mathrm{F}-Nb_\mathrm{H}=\Delta Nb_0m_0t^\beta$ using $Nb_\mathrm{J}=\Sigma_\mathrm{i}\Phi_\mathrm{i}(Nb)_\mathrm{i}$ together with $\Phi_\mathrm{F}-\Phi_\mathrm{H}=m_0t^\beta$; here Nb_J (J=F,H) is the scattering length density of each bulk liquid phase. The resulting value $A=4.51\times10^{-6}$ Å^{-2} has used throughout. $\beta/\nu=0.52$ is used, which is close to the theoretical value $\beta/\nu=\mu^\mathrm{th}=0.516$. Equation (2) is employed at distances into the interface beyond the primary adsorbed layer. The value of c is related to a universal ratio $P_0/P_\infty=c^{\nu/\beta}$. Optical experiments

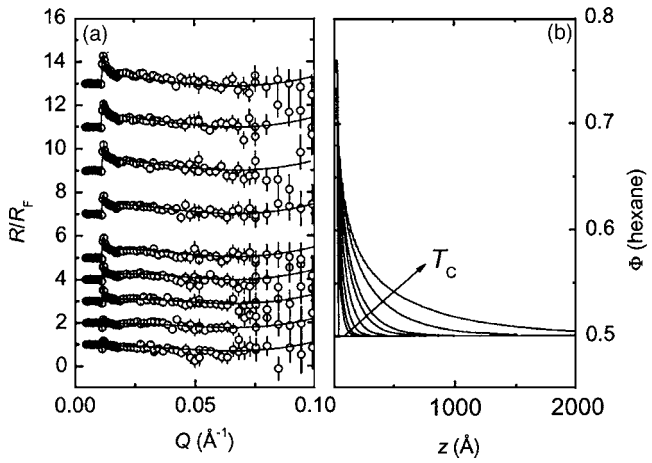

FIG. 2. (a) Normalized reflectivity data R/R_F measured as the critical point is approached for the near-critical mixture of hexane-d_{14} perfluorohexane adsorbing to the octadecyl-coated substrate. R_F is the calculated Fresnel reflectivity of the bare silicon-liquid mixture interface. From bottom to top: $t=5.32\times10^{-2}$, 2.71×10^{-2}, 1.87×10^{-2}, 1.05×10^{-2}, 5.46×10^{-3}, 2.68×10^{-3}, 1.70×10^{-3}, 5.56×10^{-4}, and 1.74×10^{-4}. The second to the fifth sets have each been shifted upwards by $R/R_F=1$ from its predecessor; the sixth to the ninth sets have each been shifted upwards by $R/R_F=2$ from its predecessor. Data points are only shown to $Q=0.1$ Å^{-1}, but in most cases measurements were made out to $Q=0.15$ Å^{-1}. Solid lines are fits according to Eq. (2). (b) Volume fraction composition profile corresponding to the fit lines shown in (a). Details of the model are given in the text and summarized in Table I.

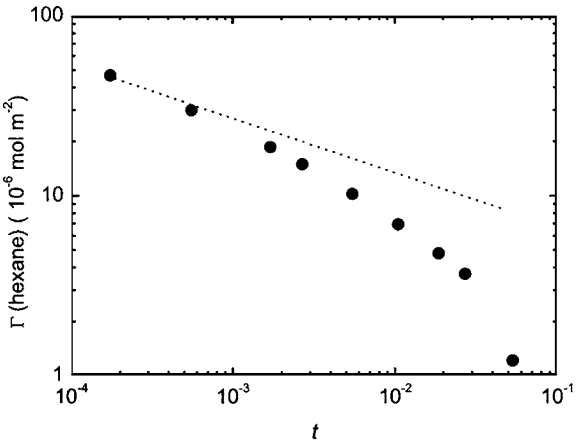

FIG. 3. Surface excess of hexane-d_{14} determined from the profiles shown in Fig. 2(b). The dotted line corresponds to the expected slope for the scaling relation $\Gamma \sim t^{-0.305}$.

[5] are consistent with $P_0/P_\infty = 0.90 \pm 0.24$ giving $c = 0.95 \pm 0.14$. However, in our modelling we find that the quality of the fit is insensitive to the choice of c ($c = 1.0 \pm 0.5$ is acceptable for the range of temperatures studied). In the analysis we have thus arbitrarily used the accepted value $c = 0.95$. In order to obtain good quality fits to the reflectivity data z_e, is used as a fitting parameter. The extrapolation length, z_e, can be determined [13] for the situation where $\xi \gg z_e$. However, the required values of $z_e \sim 65 \pm 5$ Å close to T_C and $\sim 50 \pm 10$ Å further from T_C are considerably larger than the expected values of $z_e \sim 10$ Å. It is possible that the origin of this discrepancy may arise from either the complex nature of the overall substrate surface or from the accommodation of a primary adsorbed layer (ad-layer) local to the substrate surface of varying composition and thickness. This latter suggestion is appealing since if z_e is chosen to have the same magnitude as the summation of the thicknesses of the silicon oxide, octadecyl, and ad-layer used in the modelling good model fits to the reflectivity data are obtained; the larger z_e at smaller t, may be attributed to the ad-layer increasing in thickness. The correlation length amplitude that produces consistent fits over the t range studied is $\xi_0 = 2.4 \pm 0.2$ Å, which is consistent within error with the literature values [19,36–38]; $\xi_0 = 2.4$ Å has been employed throughout. The resulting reflectivities calculated using this scaling law with these parameters are shown as the solid lines in Fig. 2(a) with the corresponding volume fraction composition profiles shown in Fig. 2(b). Earlier work on adsorption from hexane-perfluorohexane mixtures to octadecyl-coupled surfaces suggests that the surface is not 100% saturated in the preferentially adsorbed component [26,27]. However, the fact that the $P(x)$ used here adequately models the data suggests that despite the lack of complete saturation strong critical adsorption is attained. Figure 3 shows the surface excess of hexane evaluated at each t as determined from the composition profiles. The $\Gamma \sim t^{-0.305}$ behavior is only evident at small t. Curiously this contrasts with the range over which the $\Gamma \sim t^{-0.305}$ behavior is found in ellipsometry experiments for liquid-vapour interfaces [8]. In the ellipsometry measurements the measured ellipticity is corrected for a background term that accommodates the capillary-wave contribution and the sharp liquid–vapor interface. However, in the analysis of the neutron reflectivity data the analogous "background" effects (primary adsorption and surface roughness) are accommodated directly in the modeling. This difference in behavior could be related to the experiments being conducted at a solid-liquid interface, with reasons as suggested for the z_e behavior plausibly attributed to either the nature of the overall substrate surface or to a variable thickness and/or composition of the primary adsorbed layer.

Jestin *et al.* [19] have analyzed the neutron-reflection-determined composition profiles of three critical mixtures including hexane-perfluorohexane adsorbing to its free surface, as opposed to a chemically modified solid surface as in this work, and have tested the universality of the critical adsorption profile. They conclude that the high quality fits to the data validates the Liu-Fisher [5] profile [Eq. (1)]. However, they report a high value of $c = 1.68 \pm 0.4$ for the hexane-perfluorohexane system at the free surface. A relatively large extrapolation length of 23.7 Å is required in the modelling for the hexane-perfluorohexane system at the free surface, which contrasts sharply with the 3.36 Å used for methanol-cyclohexane.

B. Dietrich-Schack analysis

Neutron reflection has been employed to examine various aspects of critical adsorption by Zhao *et al.* [22] who associated a discontinuity found in the reflectivity near the critical edge with power-law decay. However, unfortunately some ambiguity in the value of the exponent describing the power-law decay remained. The exponent μ of the algebraic decay, $m(z) \sim z^{-\mu}$, can be *uniquely* determined (for $\mu < 2$), as can the magnitude of the amplitude P_0, using the method of Dietrich and Schack [28]. Essentially, if the potential that the neutrons experience decays as $V(z) = \lambda z^{-\mu}$, the values of λ and μ can be determined. This analysis has been discussed in earlier work and has demonstrated that the expected exponent $\mu^{th} = 0.516 \pm 0.004$ is consistent with experimental measurements of the critical adsorption profile [20]. Here the method of analysis is applied to an extended temperature region, over which, assuming isotopic substitution does not significantly alter it, the correlation length is known, allowing the generality and range of applicability of the theory to be further examined. If $y = \ln(1-R)$, where R is the reflectivity, is plotted against $x = E^{0.5-1/\mu'}$, where $E = (1/4)(Q^2 - Q_C^2)$, a linear function is obtained as $x \to \infty$ for a value μ' that determines an optimum $\mu = \mu'$. The range over which $y(x)$ is linear is constrained to the range $E_- \leqslant E \leqslant E_+$ where the E_+ limit is influenced by the region of E over which the asymptotic behavior of the theory is applicable and/or corrections to the leading term of the power law decay become relevant. Finite temperature resolution, the contribution to the reflectivity from the exponentially decaying part of the profile, and instrument resolution define the limit E_-. Figure 4 shows the result of this analysis; to keep the data on the same scale the data are plotted for $\mu' = 0.516$. As can be seen, linear plots are obtained. Two features are apparent from Fig. 4: the magnitude of the slope decreases and the location of

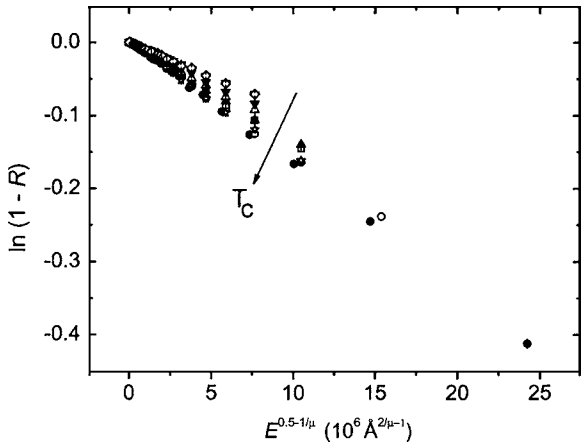

FIG. 4. Plots of $\ln(1-R)$ vs $E^{0.5-1/\mu'}$ for the common choice $\mu=0.516$ for the reflectivity data shown in Fig. 2(a). The plots show how E_- limit (at large x values) and slope of the plot, and hence determined value of P_0, varies with t. From top to bottom: $t=5.32\times10^{-2}$ (◇), 2.71×10^{-2} (▽), 1.87×10^{-2} (▼), 1.05×10^{-2} (△), 5.46×10^{-3} (▲), 2.68×10^{-3} (□), 1.70×10^{-3} (☆), 5.56×10^{-4} (○), and 1.74×10^{-4} (●).

the E_- cutoff increases (i.e., shifts to smaller x) with increasing t. The instrument and temperature resolution alone cannot justify the variable E_- limit, suggesting that the increasing prevalence of the exponential decay defines the E_- limit. Comparison of Figs. 3 and 4 reveal a notable coincidence between the t at which these features become apparent and the t at which $\Gamma\sim t^{-0.305}$ behavior is not obtained, thus highlighting the range over which the pure power-law critical adsorption profile is dominant.

For a given μ' the slope of the y vs x plot can be used to determine the magnitude of the amplitude λ and hence the value of $P_0{}'$ [28]. For the optimum $\mu=\mu'$, the corresponding optimum $P_0=P_0{}'$ can be obtained. The strength of the potential, λ, is determined via $\lambda=|(dy/dx)/2I(\mu)|^{\mu}$ where $I(\mu)$ is Dietrich and Schack's universal function [Eq. (5) in Ref. [28]]. P_0' is then determined through $P_0'=\lambda/(4\pi N b_0 \xi_0^{\mu})$, with the optimum value of $\mu=\mu'$ yielding the optimum $P_0=P_0'$. We consider first analysis of the reflectivity data measured closest to T_C. Figure 5 shows the relationship between $P_0{}'$ and μ'. Data are shown for two different E_- cutoffs. Although the choice of E_- cutoff, if not selected appropriately, can lead to higher-than-expected values of the optimum μ', there is very little impact on the $P_0{}'$ over the range of acceptable μ', i.e., those μ' that yield a linear plot. The uncertainties in evaluated P_0' values are dominated by the uncertainty in the value of ξ_0. The obtained $\mu'=0.505\pm0.025$ is in agreement with $\mu^{\rm th}=0.516\pm0.004$. The resulting optimum μ' and $P_0{}'$ are those given in Figs. 6(a) and 6(b) for the lowest t. The optimum $P_0'=0.90\pm0.04$ obtained is close to the theoretical value $P_0^{\rm th}=0.94\pm0.05$ and the experimentally determined value $P_0^{\rm ex}=0.955\pm0.08$ [13] and $P_0^{\rm MC}=0.866$ determined from Monte Carlo simulations [39]. The error boxes on Fig. 5 illustrate the extent of agreement.

However, the t dependence of the slope (Fig. 4) has an impact on the value of P_0 that can be determined from this data analysis if the mixture is not sufficiently close to T_C.

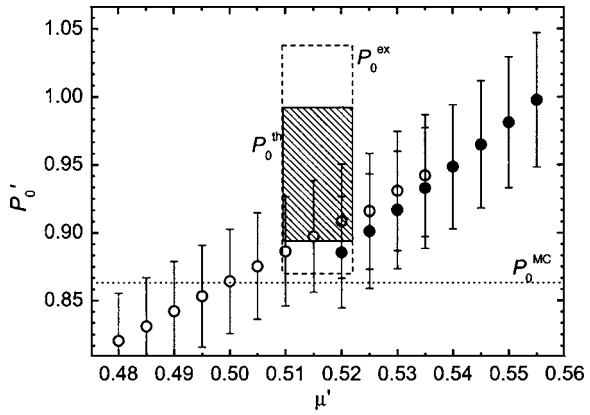

FIG. 5. Variation in P_0' with choice of μ' for $t=1.74\times10^{-4}$, the closest temperature to T_C. Two different E_- cutoffs have been employed to demonstrate the variation in P_0' this induces. For the open circles the E_- cutoff is 7.32×10^{-6} Å^{-2} and for the filled circles 4.39×10^{-6} Å^{-2}. The boxes show the experimental (open) and theoretical (hatched) ranges of P_0.

The t dependence of μ' and $P_0{}'$ are shown in Figs. 6(a) and 6(b), respectively. The value of μ' (=μ) is essentially independent of temperature, and is 0.514 ± 0.018, which is in good agreement with $\mu^{\rm th}$. As expected from the variation in the slope of the plot, $P_0{}'$ is temperature dependent. The attainment of the limiting value for $t\to0$ of 0.90 ± 0.04 is coincident with the onset of the $\Gamma\sim t^{-0.305}$ behavior discussed earlier.

Our value of P_0 determined using Dietrich and Schack's method is in excellent agreement with the theoretical value and in contrast to experimentally determined values by Jestin *et al.* who report a large value of $P_0=1.78\pm0.20$. Strong adsorption is the proposed origin of this discrepancy. Howse *et al.* [20] applied the theory of Dietrich and Schack to a near-critical mixture of 2-butoxyethanol+D_2O close to T_C revealing the exponent describing the power law decay to be

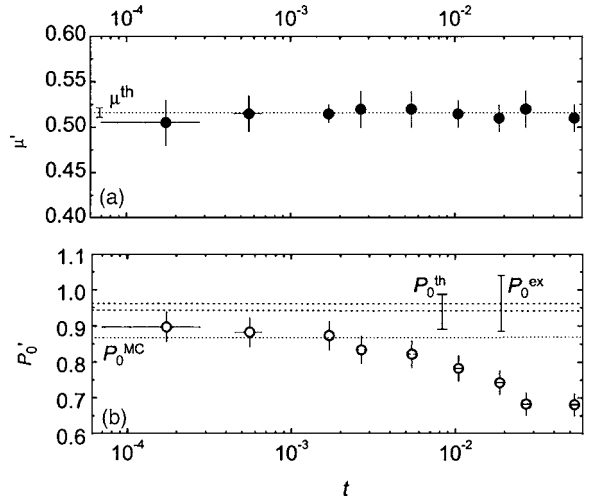

FIG. 6. (a) Evaluated optimum μ'(=μ) as a function of t after appropriate choice of the E_- cutoff. (b) Evaluated P_0 for each μ as a function of t. Error bars are shown that correspond to appropriate theoretical and experimental determinations of these parameters.

in agreement with the theoretical value. Similar results were obtained for a related system [23]. However, the determined value of P_0 was unreasonably low. Here, we have demonstrated that this method of analysis can yield satisfactory values for μ and P_0. From the Dietrich-Schack analysis the power-law decay has been examined and within experimental uncertainty the exponent obtained is in agreement with the theoretical value. For $\xi < 150$ Å it appears that the exponential decay becomes significant enough to influence the E_- limit and also the determined value of P_0. This is a significant point for the consideration of the crossover regime from critical adsorption to complete wetting for which exponentially decaying profiles are found to be suitable models. In the off-critical region it is unlikely that the correlation length reaches this magnitude and the critical adsorption power-law decay is suppressed.

IV. SUMMARY

Neutron reflectometry has been employed to examine critical adsorption composition profiles. The analysis method of Dietrich and Schack [28] has been applied to examine the nature of the power law, $z^{-\mu}$, section of the critical adsorption composition profile. Values of $\mu = 0.514 \pm 0.018$ and $P_0 = 0.90 \pm 0.04$ have been obtained, both of which are consistent with theoretical expectations ($\mu^{\text{th}} = 0.516 \pm 0.004$; $P_0^{\text{th}} = 0.94 \pm 0.05$, $P_0^{\text{MC}} = 0.866$) and other experimental determinations ($P_0^{\text{ex}} = 0.955 \pm 0.08$).

ACKNOWLEDGMENTS

This research project has been supported by the European Commission under the 6th Framework Programme through the Key Action: Strengthening the European Research Area, Research Infrastructures, Contract No. RII3-CT-2003-505925 (NMI3). The authors wish to thank BENSC for allocation of beamtime and access to support and facilities, and Bruce Law for helpful correspondence.

[1] B. M. Law, Prog. Surf. Sci. **66**, 159 (2001).
[2] D. Bonn and D. Ross, Rep. Prog. Phys. **64**, 1085 (2001).
[3] M. E. Fisher and P. G. De Gennes, C. R. Seances Acad. Sci., Ser. B **287**, 207 (1978).
[4] J. S. Rowlinson and B. Widom, *Molecular Theory of Capillarity* (Dover, Mineola, NY, 2002).
[5] A. J. Liu and M. E. Fisher, Phys. Rev. A **40**, 7202 (1989).
[6] G. Flöter and S. Dietrich, Z. Phys. B: Condens. Matter **97**, 213 (1995).
[7] D. S. P. Smith and B. M. Law, Phys. Rev. E **52**, 580 (1995).
[8] D. S. P. Smith and B. M. Law, Phys. Rev. E **54**, 2727 (1996).
[9] D. S. P. Smith and B. M. Law, J. Chem. Phys. **99**, 9836 (1993).
[10] C. L. Caylor and B. M. Law, J. Chem. Phys. **104**, 2070 (1996).
[11] J. H. Carpenter, B. M. Law, and D. S. P. Smith, Phys. Rev. E **59**, 5655 (1999).
[12] J. H. Carpenter, J.-H. J. Cho, and B. M. Law, Phys. Rev. E **61**, 532 (2000).
[13] D. S. P. Smith, B. M. Law, M. Smock, and D. P. Landau, Phys. Rev. E **55**, 620 (1997).
[14] Jae-Hie J. Cho and B. M. Law, Phys. Rev. E **65**, 011601 (2002).
[15] N. S. Desai, S. Peach, and C. Franck, Phys. Rev. E **52**, 4129 (1995).
[16] J.-H. J. Cho and B. M. Law, Int. J. Thermophys. **25**, 1449 (2004).
[17] J.-H. J. Cho and B. M. Law, Phys. Rev. Lett. **86**, 2070 (2001).
[18] J.-H. J. Cho, B. M. Law, and K. Gray, J. Chem. Phys. **116**, 3058 (2002).
[19] J. Jestin, L.-T. Lee, M. Privat, and G. Zalzer, Eur. Phys. J. B **24**, 541 (2001).
[20] J. R. Howse, J. Bowers, E. Manzanares-Papayanopoulos, I. A. McLure, and R. Steitz, Phys. Rev. E **59**, 5577 (1999).
[21] L. W. Marschand, M. Brown, L. B. Lurio, B. M. Law, S. Uran, I. Kuzmenko, and T. Gog, Phys. Rev. E **72**, 011509 (2005).
[22] H. Zhao, A. Penninckx-Sans, L.-T. Lee, D. Beysens, and G. Jannink, Phys. Rev. Lett. **75**, 1977 (1995).
[23] J. R. Howse, E. Manzanares-Papayanopoulos, I. A. McLure, J. Bowers, R. Steitz, and G. H. Findenegg, J. Chem. Phys. **116**, 7177 (2002).
[24] M. M. Telo da Gama and U. M. B. Marconi, Physica A **171**, 69 (1991).
[25] S. B. Kiselev, J. F. Ely, and M. Y. Belyakov, J. Chem. Phys. **112**, 3370 (2000).
[26] J. Bowers, A. Zarbakhsh, H. K. Christenson, I. A. McLure, and R. Cubitt, J. Chem. Phys. **119**, 11917 (2003).
[27] J. Bowers, A. Zarbakhsh, A. Querol, H. K. Christenson, I. A. McLure, and R. Cubitt, J. Chem. Phys. **121**, 9058 (2004).
[28] S. Dietrich and R. Schack, Phys. Rev. Lett. **58**, 140 (1987).
[29] J. Penfold, R. M. Richardson, A. Zarbakhsh, J. R. P. Webster, D. G. Bucknall, A. R. Rennie, R. A. L. Jones, T. Cosgrove, R. K. Thomas, J. S. Higgins, P. D. I. Fletcher, E. Dickinson, S. J. Roser, I. A. McLure, A. R. Hillman, R. W. Richards, E. J. Staples, A. N. Burgess, E. A. Simister, and J. W. White, J. Chem. Soc., Faraday Trans. **93**, 3899 (1997).
[30] C. Braun, Parratt32 fitting routine for reflectivity data, Hahn-Meitner-Institut, Berlin, 1997–1999.
[31] L. G. Parratt, Phys. Rev. **95**, 359 (1954).
[32] M. S. B. Munson, J. Phys. Chem. **68**, 796 (1964).
[33] I. A. McLure, A. Mohktari, and J. Bowers, J. Chem. Soc., Faraday Trans. **93**, 249 (1997).
[34] F. Wegner, Phys. Rev. B **5**, 4529 (1972).
[35] R. G. Bedford and R. D. Dunlap, J. Am. Chem. Soc. **80**, 282 (1958).
[36] J. Schulz, A. Hirtz, and G. H. Findenegg, Physica A **244**, 334 (1997).
[37] G. I. Pozharskaya, N. L. Kasapova, V. P. Skripov, and Y. D. Kolpakov, J. Chem. Thermodyn. **16**, 267 (1984).
[38] I. A. McLure and P. J. Clements, Ber. Bunsenges. Phys. Chem. **101**, 114 (1997).
[39] M. Smock, H. W. Diehl, and D. P. Landau, Ber. Bunsenges. Phys. Chem. **98**, 486 (1994).